

# Goldilock rules, Quantum cellular automata and coarse-graining

O. Duranthon<sup>1</sup> and Giuseppe Di Molfetta<sup>2,\*</sup>

<sup>1</sup>*Aix-Marseille Université, CNRS, Laboratoire d'Informatique et Systèmes, Marseille, France and Département de physique, Ecole Normale Supérieure, Paris, France*

<sup>2</sup>*Aix-Marseille Université, CNRS, Laboratoire d'Informatique et Systèmes, Marseille, France*

(Dated: July 13, 2022)

One can think of some physical evolutions as being the emergent-effective result of a microscopic discrete model. Inspired by classical coarse graining procedures, we provide a simple procedures to coarse-grain color-blind quantum cellular automata, following Goldilock rules. The procedure consists in (i) space-time grouping the quantum cellular automaton (QCA) in cells of size  $N$ , (ii) projecting the cells states onto its borders, connecting them with the fine dynamics, which is reminiscent of the edge-bulk correspondence in quantum field theory; (iii) describe the overall dynamics by the border states, that we call signals; (iv) construct the coarse-grained dynamics for different sizes  $N$  of the cells. A byproduct of this simple toy-model is a general discrete analogous of the Stokes law. Moreover, we proved that in the spacetime limit, the automaton converge to a Dirac free Hamiltonian. The QCA we introduced here, can be implemented by present-day quantum platforms, such as Rydberg arrays, trapped ions, and superconducting qubits. We hope our study can pave the way to a richer understanding of those systems with limited resolution.

## I. INTRODUCTION

Cellular automata are discrete dynamic systems whose rules appear very simple, but whose emerging phenomenology is complex [1]. An example is Conway's famous Game of life [2] : simple understandable rules produce an entire animated world, with blinkers, gliders, guns, Garden of Eden states. Historically, they have been adapted to describe several complex systems such as hydrodynamic fluids [3], traffic patterns [4], the formation of biological processes [5] and reaction-diffusion [6]. One of the first definitions of cellular automata is that of von Neumann [7], whose rules are applied locally on a two-dimensional grid, in discrete time. It soon became clear that many CA are universal calculation models, or in other words they effectively simulate Turing machines [8]. More formally CA are discrete set of cells whose values are in identical finite sets ; a state is the current value of the cells ; cells evolve in discrete time according to a local translation-invariant update rule.

Although cellular automata describe a very broad spectrum of classical phenomena, they cannot describe a quantum system. In order to do so correctly and effectively, to the best of our knowledge today, we must consider the quantum analogue of CA, namely quantum cellular automata (QCA)[9, 10]. Quantum cellular automata are quantization of the classical CA. They can be defined in various ways, and many of them are recently proved equivalent [9].

We define our QCA over a general graph where in each vertex sits a cell, with each cell composed of sub-cells defined as finite dimensional quantum systems. The evolution of the QCA is given by local unitaries that act on partitions of the graph. From the above definition it is clear that all quantum cellular automata in this model are reversible, as only unitary operations are performed. This is in accordance with the expected microscopic, fully quantum, dynamics.

These automata can be used as a model of distributed quantum computation and in particular they can provide quantum schemes to simulate quantum physics theories [11–14]. Indeed QCA offer a natural framework to theoretical physics. They seem promising since they satisfy fundamental concepts such as unitarity and causality, and we can make them gauge invariant [15–17] or Lorentz covariant [18–20].

If a quantum description of a discrete dynamic system does not pose major problems, the transition to classical is not yet free of difficulties.

Here we propose to depart from the discrete structure of the QCA, to obtain emergent classical or semi-classical dynamics, by coarse-graining the system. The idea of coarse-graining complex systems other than particles or polymers is very recent, and range from quantum chemistry [21] and high energy physics [22–24] to biology [25].

Here, inspired by classical coarse graining procedures [26, 27], we space-time group many unit cells and time steps in one supercell, and we construct effective emergent dynamics for different sizes of the supercell. In the most low-level we have the fully microscopic and reversible quantum dynamics ; while for increasing supercell size the quantum features are gradually suppressed and a non-reversible dynamic emerge.

With this procedure we can investigate whether a classical dynamic will emerge, or if the quantum fluctuations of the fundamental local observables are sizeable throughout the coarse graining, thus not allowing for its classical simulation. Note that this procedure, together with the continuous limit of the QCA dynamics, can be used to obtain master equations for the system's dynamics. These equations are however for the closed system, and the loss of information comes strictly from the description level – one can imagine that the available “detectors” are not good enough to resolve the more basic level of the dynamics, and as such it only makes sense to speak of a high-level description.

We are thus proposing a way to obtain effective dynamics for closed quantum systems for which a complete description is not available. In particular we will describe the system at different scales and in different levels of detail, as if one would

\*Electronic address: giuseppe.dimolfetta@lis-lab.fr

zoom out from the microscopic description.

The use of QCA is particularly useful for a coarse graining procedure, as its discrete structure gives a clear visualization of the process : instead of being able to resolve a single cell, one is only able to see bigger blocks, thus not taking into account the full information about the microscopic structure. This erasure of information will lead to an effective state and effective dynamics, which will be possibly simpler than the microscopic fully quantum dynamics and thus, at some level, likely to be simulated in an efficient way by a classical computer.

We will specialise the above idea, by applying it to a very broad class of QCAa, following Goldilock rules, recently introduced in [28]. Goldilock rules are trade-offs of the kind underpinning biological, social, and economic emergent complexity. For a sake of simplicity, we will investigate the simplest, but still non trivial, rule which makes the state evolution depending on a neighbourhood of unitary radius. The interest for such a choice is double : (i) as it will be proven, this Goldilock QCA is color-blind, i.e. is global invariant under the change  $0 \leftrightarrow 1$ ; (ii) the overall dynamics may be described by borders-states, we call *signals*, leaving on the edges of the grid. We will see that these signals are natural candidates for describing the QCA at different level description. In particular, in order to study the emergent macroscopic dynamics, we partition the spacetime diagram in cells of different sizes and then we describe the cell-borders dynamics using a discrete analogous of Stokes law. Finally we coarse-grain the border-states, namely the signals, to recover a higher-level description.

## II. GOLDILOCKS RULES

In this section, we introduce the model, namely the Goldilocks QCA (GQCA) over a one-dimensional qbit strings, depicted in Fig. 1. Each qbit  $|e_i\rangle \in \mathbb{C}^2$ , updates in discrete time steps, according to a local gate defined on the qbit's neighborhood as follows:

$$U_i = \sum_{\sigma=e_{i-1},e_{i+1}} |\sigma\rangle\langle\sigma| \otimes V_i^{c_\sigma}.$$

where  $U_i$  and  $V_i$ , are local unitary gates, acting on the qbit at position  $x_i$ , and the sum is performed on the four possible configurations  $\sigma$  of the two neighbors of  $i$ . The parameter  $c_\sigma \in \{1, 0\}^2$  controls weather  $V_i$  is applied or not to  $|e_i\rangle$ . According to the simplest Goldilocks rule  $T_1$  [28], we have to apply  $V$  to  $|e_i\rangle$  if its two neighbors are different, otherwise we have to keep it unchanged, leading to the following rule :  $c_{00} = 0$ ,  $c_{11} = 0$ ,  $c_{01} = 1$  and  $c_{10} = 1$ .

The dynamics of the GQCA strongly depends on the choice of  $V$ . A sufficiently general expression for  $V$  is the following:

$$V = e^{i\phi}(\cos(m\varepsilon)\sigma_x + \sin(m\varepsilon)\sigma_z), \quad (1)$$

where  $\phi \in [0, 2\pi[$  and  $m$  is a constant real parameter, which we call the *mass*. The real parameter  $\varepsilon$  is the characteristic length of the grid.

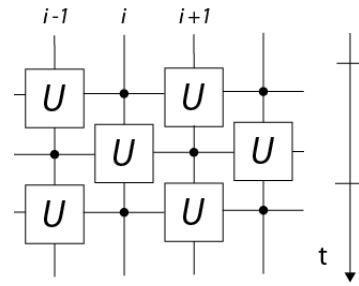


FIG. 1: The GQCA in one spatial dimension. Squares represents local unitary gates  $U$  applied to a qbit state.

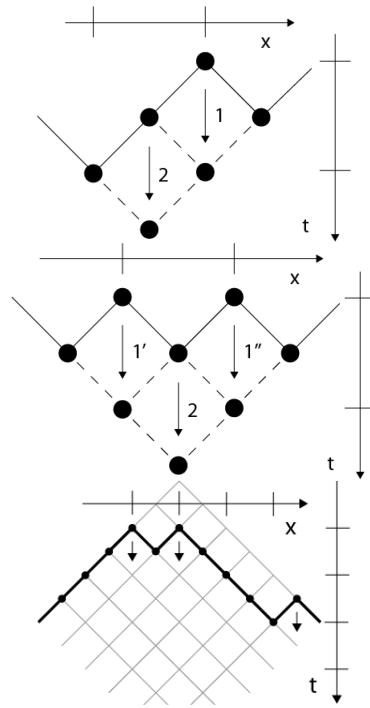


FIG. 2: The looser evolution rule : *left* we can evolve 1, via unitary transformation  $U_1$ , then 2, via  $U_2$  ; *right* we can evolve 1', via  $U_{1'}$  and 1'', via  $U_{1''}$ . *Bottom* the bold line is the current state.

One may remark that the scheme depicted in Fig.1, still well defined, does not put time and space on an equal footing, because we apply first gates at odd positions at time  $t_j$  and later gates at even positions at time  $t_j + 1/2$ . To avoid this inconvenient, we can equivalently represent the GQCA, depicted in Fig.1, as in Fig.2. Since the unitaries  $U_i$  and  $U_j$  commute if  $|i - j| > 1$ , we say that the state at position  $x_i$  and time  $t_j$  can evolve to the position  $x_i$  at time  $t_j + \varepsilon$ , if its two neighbors  $x_i - \varepsilon$  and  $x_i + \varepsilon$  are ahead at time  $t_j + \varepsilon/2$ . In Fig.2, the black solid arrows represent the local time evolution of the state and the current state is then represented by a broken solid line.

The dynamics of a GQCA locally looks very simple, as it is shown in Fig.3 and Fig.5, although at large scale it may lead to high complexity [28]. In fact, by looking at its space-

time diagram, we can observe finite regions of  $|0\rangle$ s and  $|1\rangle$ s propagating quite regularly. In this scenario, the *domain walls* between these regions, appear to be the most relevant point to investigate. This suggests a dual representation of the GQCA. Let us introduce an auxiliary qbit  $\psi \in \mathbb{C}^2$ , sitting on the edges

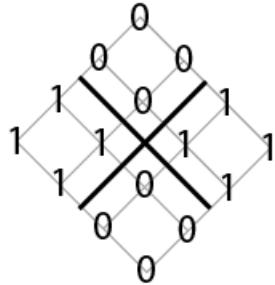


FIG. 3: The time evolution of the GQCA and the domain walls (bold lines) with  $\phi = 0$  and  $m = 0$ .

of the space-time grid : this new discrete field is defined in order to account, modulo 2, the local difference between the qbits  $|0\rangle$ s and  $|1\rangle$ s of two nearest neighbor qbits. If they are different,  $\psi = |1\rangle$ , otherwise  $\psi = |0\rangle$ , or more formally:

$$\psi(x_i + \varepsilon/2, t_i + \varepsilon/2) = e(x_i, t_i) \oplus e(x_{i+1}, t_{i+1}).$$

As we can see in Fig. 4, the  $\bar{\psi} \equiv |1\rangle$  recovers a special role in describing the dynamics and seems propagate in space-time, with limiting speed 1, following the domain walls that separate regions of  $|0\rangle$ s and  $|1\rangle$ s.

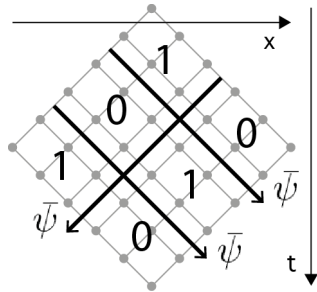


FIG. 4: The time evolution of the  $\bar{\psi}$ s (bold lines)

We can fully describe the automaton only looking at the signal  $\bar{\psi}$ , which singularly behaves like a quantum walker over the dual grid. Indeed, if we look at the one  $\bar{\psi}$ -subspace, a straightforward calculation leads us to the following recursive relations:

$$\begin{aligned} \bar{\psi}^+(t + \frac{1}{2}, x) &= \cos(\varepsilon m) \bar{\psi}^+(t, x - \frac{1}{2}) \pm \sin(\varepsilon m) \bar{\psi}^-(t, x - \frac{1}{2}) \\ \bar{\psi}^-(t + \frac{1}{2}, x) &= \cos(\varepsilon m) \bar{\psi}^-(t, x + \frac{1}{2}) \mp \sin(\varepsilon m) \bar{\psi}^+(t, x + \frac{1}{2}) \end{aligned} \quad (2)$$

where  $\bar{\psi}^+$  (resp.  $\bar{\psi}^-$ ) the right (resp. left) signal and the sign choice depends whether we have  $0 - \bar{\psi} - 1$  or  $1 - \bar{\psi} - 0$ . The parameter  $m$  plays the role of a mass term, or alternatively may be seen as the reflectance of  $V$ .

The constant  $\phi$  selects the signals statistics : when two  $\bar{\psi}$ s cross, we obtain a phase delay of  $2\phi$  and this phase induces a statistics. For  $\phi = \pi/2$ , the  $\bar{\psi}$ s have to be considered fermions. The local evolution rules for  $\bar{\psi}$  are summarised in Fig. 5.

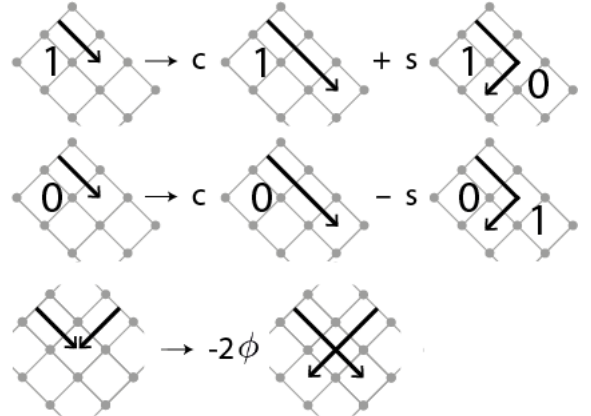


FIG. 5: One time step evolution rules of  $\bar{\psi}$ . A  $-2\phi$  means a phase delay in the complex phase.

This paves the way to interesting new perspectives in the understanding of the mathematical complexity of the Goldilocks QCA. The fact that the signals  $\bar{\psi}$ s actually behaves as (Dirac) quantum walkers in (1+1) is quite surprising : quantum walker is usually though as the one-particle sector of a QCA. The reason seems to be that the domain walls, although defined in a multi-particle setting, behave geometrically as one dimensional states.

### III. COLOR BLINDNESS

Color-blind cellular automata have been extensively studied in [29], where all cells get transformed by the same group element. The quantum analogue has not been studied to the best of our knowledge. Although a complete characterization of this class of automata goes beyond the scope of this manuscript, we will demonstrate in this section that our GQCA is color-blind and therefore subject to a global gauge invariance under transformation  $0 \leftrightarrow 1$ .

Let us consider the gates

$$U_i = \sum_{s=e_{i-1}, e_{i+1}} |s\rangle\langle s| \otimes V_i^{c_s},$$

with the same Goldilocks rules for  $c_s$  we introduced. The most general unitary for the gate  $V$  reads

$$V = \begin{pmatrix} a & b \\ -e^{i\phi}b^* & e^{i\phi}a^* \end{pmatrix}$$

with  $a = |a|e^{i\alpha}$ ,  $b = |b|e^{i\beta}$ ,  $|a|^2 + |b|^2 = 1$  and  $\phi$  real.

Now, we compare the evolution of the signal  $\bar{\psi}$  in the two possible gauges. Either the gauge is  $0 - \bar{\psi} - 1$  and the evolution

is:

$$\begin{smallmatrix} 0 & 1 & 1 \\ 0 & 0 & 1 \end{smallmatrix} \xrightarrow{U_{2i}} \begin{smallmatrix} 0 & 1 & 1 \\ 0 & 0 & 1 \end{smallmatrix} + e^{i\phi} a^* \begin{smallmatrix} 0 & 1 & 1 \\ 0 & 1 & 1 \end{smallmatrix};$$

either it is  $1 - \bar{\psi} - 0$  and the evolution is:

$$\begin{smallmatrix} 1 & 0 & 0 \\ 1 & 0 & 0 \end{smallmatrix} \xrightarrow{U_{2i}} -e^{i\phi} b^* \begin{smallmatrix} 1 & 0 & 0 \\ 1 & 1 & 0 \end{smallmatrix} + a \begin{smallmatrix} 1 & 0 & 0 \\ 1 & 0 & 0 \end{smallmatrix}.$$

We summarize these rules as :

$$0 - \bar{\psi}^+(x, t) - 1 \rightarrow b\bar{\psi}^+(x+1, t+1) + e^{i\phi} a^* \bar{\psi}^-(x-1, t+1),$$

$$0 - \bar{\psi}^-(x, t) - 1 \rightarrow a\bar{\psi}^+(x+1, t+1) - e^{i\phi} b^* \bar{\psi}^-(x-1, t+1);$$

or in the second gauge

$$1 - \bar{\psi}^+(x, t) - 0 \rightarrow -e^{i\phi} b^* \bar{\psi}^+(x+1, t+1) + a\bar{\psi}^-(x-1, t+1),$$

$$1 - \bar{\psi}^-(x, t) - 0 \rightarrow e^{i\phi} a^* \bar{\psi}^+(x+1, t+1) + b\bar{\psi}^-(x-1, t+1).$$

Notice that the change  $0 \leftrightarrow 1$  induces only phase shifts on transition rates and preserves their amplitudes. There are only four possible phase shifts if we change the gauge from  $0 - \bar{\psi} - 1$  to  $1 - \bar{\psi} - 0$  : (i)  $\Delta\varphi_1 = 2\alpha - \phi$  for  $\bar{\psi}^+ \rightarrow \bar{\psi}^-$  ; (ii)  $-\Delta\varphi_1$  for  $\bar{\psi}^- \rightarrow \bar{\psi}^+$  ; (iii)  $\Delta\varphi_2 = 2\beta - \phi + \pi$  for  $\bar{\psi}^- \rightarrow \bar{\psi}^-$  and (iv)  $-\Delta\varphi_2$  for  $\bar{\psi}^+ \rightarrow \bar{\psi}^+$ .

Now, let us look, first, to the single signal subspace : the total phase shift does not depend on the particular trajectories, meaning that the motion of one signal is gauge-invariant. We prove it in the following.

The initial state is  $\bar{\psi}^c(x, t)$ , the final state is  $\bar{\psi}^q(x+N, t+T)$  with  $c, q = \pm$  and  $N \in \{-T, -T+2, \dots, T\}$ . There are  $n^+$  times  $\bar{\psi}^+ \rightarrow \bar{\psi}^-$  and  $n^-$  times  $\bar{\psi}^- \rightarrow \bar{\psi}^+$  with  $n^+ = n^-$  if  $c = q$ ,  $n^+ = n^- + 1$  if  $c = +$  and  $q = -$  or  $n^+ = n^- - 1$  if  $c = -$  and  $q = +$  ; there are  $m^+$  times  $\bar{\psi}^+ \rightarrow \bar{\psi}^+$  and  $m^-$  times  $\bar{\psi}^- \rightarrow \bar{\psi}^-$  with  $m^+ + n^- - m^- - n^- = N$ . We change the gauge from  $0 - \bar{\psi} - 1$  to  $1 - \bar{\psi} - 0$  ; the phase shift is

$$\Delta\varphi = (n^+ - n^-)\Delta\varphi_1 + (m^- - m^+)\Delta\varphi_2 = -N\Delta\varphi_2 + \begin{cases} 0 & \text{if } c = q, \\ \Delta\varphi_1 - \Delta\varphi_2 & \text{if } c = + \text{ and } q = -, \\ \Delta\varphi_2 - \Delta\varphi_1 & \text{if } c = - \text{ and } q = + \end{cases}$$

which does not depend on a particular trajectory.

For a many signals case, the motion is gauge-invariant if

$$2(2\beta - \phi) = 0$$

and

$$2\alpha - 2\beta = \pi.$$

Consider two signals at initial time  $\bar{\psi}^{c_1}(x_1, t)$  and  $\bar{\psi}^{c_2}(x_2, t)$ ,  $x_1 < x_2$  and final time  $\bar{\psi}^{q_1}(x'_1, t+T)$  and  $\bar{\psi}^{q_2}(x'_2, t+T)$ ,  $x'_1 > x'_2$ . If the signals do not cross, nothing changes. If they

do at position  $x$  and the gauge is  $0 - \bar{\psi}_1 - 1 - \bar{\psi}_2 - 0$ , the shift reads

$$\begin{aligned} \Delta\varphi = & - (x - x_1)\Delta\varphi_2 + \begin{cases} 0 & \text{if } c_1 = + \\ \Delta\varphi_2 - \Delta\varphi_1 & \text{if } c_1 = - \end{cases} \\ & + (x - x_2)\Delta\varphi_2 - \begin{cases} 0 & \text{if } c_2 = - \\ \Delta\varphi_1 - \Delta\varphi_2 & \text{if } c_2 = + \end{cases} \\ & - (x'_2 - x + 1)\Delta\varphi_2 + \begin{cases} 0 & \text{if } q_2 = - \\ \Delta\varphi_2 - \Delta\varphi_1 & \text{if } q_2 = + \end{cases} \\ & + (x'_1 - x - 1)\Delta\varphi_2 - \begin{cases} 0 & \text{if } q_1 = + \\ \Delta\varphi_1 - \Delta\varphi_2 & \text{if } q_1 = - \end{cases} \\ = & -(x'_2 - x_1)\Delta\varphi_2 + (x'_1 - x_2)\Delta\varphi_2 - 2\Delta\varphi_2 + m(\Delta\varphi_2 - \Delta\varphi_1), \end{aligned}$$

with  $m = 0, 1, 2, 3, 4$  depending on the charges. The two first terms correspond to single signal motions ; the two last must cancel i.e.  $2\Delta\varphi_2 = 0$  and  $\Delta\varphi_2 - \Delta\varphi_1 = 0$ . Finally from the conditions (i, ii, iii, iv), we recover the two constraints  $2(2\beta - \phi) = 0$  and  $2\alpha - 2\beta = \pi$ . Notice that, these two equations imply that  $e^{i\phi} = -s_1 e^{i2\beta}$  and  $e^{i\alpha} = s_2 i e^{i\beta}$ , with  $s_1, s_2 = \pm 1$ , leading to

$$V = s_2 i e^{i\beta} \begin{pmatrix} |a| & -s_2 i |b| \\ -s_1 s_2 i |b| & s_1 |a| \end{pmatrix}. \quad (3)$$

The above gate is the one we need for keeping the signals trajectories gauge invariant. Finally observe that, the local operator introduced in Eq. (II) is of the same kind of (III), which proves that our GQCA is color-blind.

#### IV. DECIMATION AND COARSE-GRAINING

The procedure to coarse-grain the above automaton is decomposed in three steps. First we partition the space-time diagram in cells of size  $N$ . Then we sample few qubits on the borders of these cells, and we call them probes. We will see that we can always establish a connection between the probes, along the domain walls and the signals, travelling through the cells. Finally we coarse-grain, by a CPTP map, the signals, constructing the effective dynamics for different sizes of the cells.

Let us illustrate the first two points with the help of an example. Consider a space-time diamond of size  $N = 3$  and a line of seven qubits, arranged as in Fig. 6, its extremities being fixed. From a microscopic point of view, the unitary evolution of one qubit  $|e_i\rangle$  is given locally by  $U_i$ . A probe state is the result of a projection of the automaton onto some sites, say onto the vertices of the space-time diamond depicted in Fig. 6 (top-right). Its evolution can be computed applying the following stroboscopic chain of operators :

$$U_i^{cg} = U_i (U_{i-1} U_{i+1}) (U_{i-2} U_i U_{i+2}) \dots (U_{i-N+1} \dots U_{i+N-1}) \dots (U_{i-1} U_{i+1}) U_i.$$

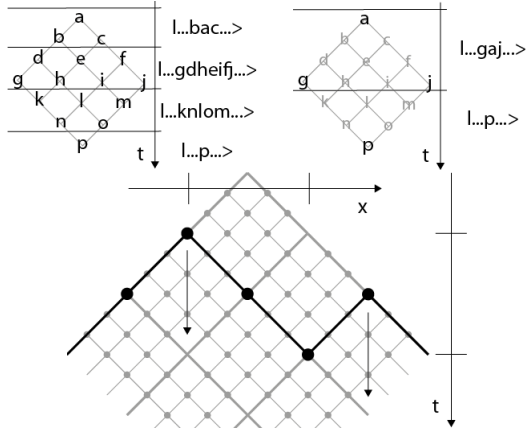


FIG. 6: *Top* Evolution and states without and with graining. The initial states are the upper ones (g, d, b, a, c, f and j).  $N = 3$ . *Bottom* the bold line is the current coarse-grained state ; we can notice the similarity between the fine state and the coarse state.

Now, whenever we have access to a probe, what can we infer about the microdynamics ? We answer this question using the dual representation of the GQCA, introduced earlier. Indeed, the auxiliary qbit  $\bar{\psi}$ , sitting on the edges of the microscopic grid, captures a local feature of the automaton. If we are able to access to the probe states, then we may have enough information to describe the microscopic dynamics.

A straightforward way is to count how many  $\bar{\psi}$ s go between two arbitrary probes, by integrating along edges modulo 2 the  $\bar{\psi}$ s, as in Fig. 7. More formally, we obtain :

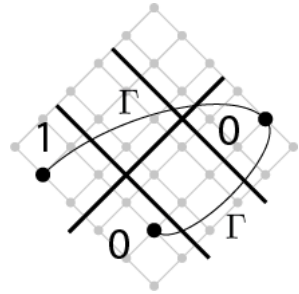


FIG. 7: Counter. The three bold dots are probes. The bold lines are the signals  $\bar{\psi}$ s. The fine lines are possible paths  $\Gamma$  that go from one probe to another one. *Top* :  $\Gamma$  encounters three  $\bar{\psi}$ s,  $3 = 1 \bmod 2$  so its two vertices have different values. *Bottom* :  $\Gamma$  encounters two  $\bar{\psi}$ s,  $2 = 0 \bmod 2$  so its two vertices have the same value.

$$e_1^{cg} \oplus e_2^{cg} = \sum_{\Gamma \text{ path from 1 to 2}} \bar{\psi} \bmod 2 = \\ = \bigoplus_{i \in \Gamma} e(x_i, t_i) \oplus e(x_{i+1}, t_{i+1}). \quad (4)$$

Note that, the above equation may be seen remarkably as a discrete analogous of Stokes formula.

Using this result, and having access to the probes, we can deduce how many  $\bar{\psi}$ s we cross going from one probe to another following a path  $\Gamma$ , as it is shown in Fig.7. In other

words, we can describe a line of fine states by its two vertices, i.e. the two probes. It turns out that this procedure coincides with a geometrical projection of the system onto its borders, which is reminiscent of the edge-bulk correspondence in quantum field theory. Also, from Eq.(IV) we may argue that parallel rays of an even number of close enough  $\bar{\psi}$ s are not seen from an hypothetical detector, as it is shown in Fig. 8. In this case the evolution of a probe does not depend on the fine state it represents.

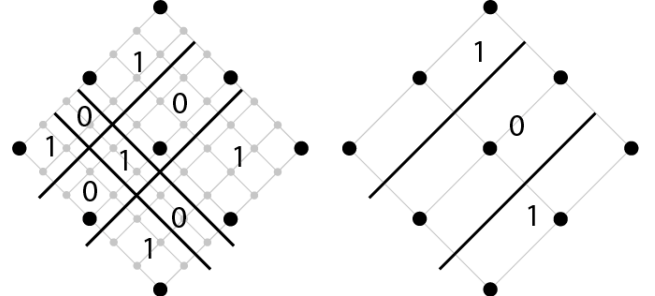


FIG. 8: Graining of the evolution. The bold dots are the probes i.e. the qubits we observe. *Left* the bold lines are the fine grained motion of the  $\bar{\psi}$ s. *Right* the probe qubits cannot catch one of the two rays made of two parallel moving  $\bar{\psi}$ s.

Finally, we coarse-grain the evolution of the signals. We consider the single signal subspace and the general Dirac-like evolution  $V = \cos(m\varepsilon)\sigma_x + \sin(m\varepsilon)\sigma_z$ . The overall dynamics for the signal  $\bar{\psi}$  is given by Eq.(II). The coarse-graining is depicted as in Fig. 9 and detailed in the Appendix VI. In concrete, we project the state on a broken line of probes separated by  $N$  fine qubits ; the signals, crossing the same edge, are not distinguishable; they are mapped onto the same coarse state.

This lack of resolution can be formalised as a CPTP map, as we detail in the Appendix. The idea is the following : let us consider a fine state composed by two qubits  $|ef\rangle$ , and its density matrix  $\rho = |ef\rangle\langle ef|$ . If our "detector" is not good enough to distinguish, e.g., the states  $|01\rangle$  and  $|10\rangle$ , then these states will be mapped to the same coarse-state in the higher-level description. More formally, we apply a CPTP map  $\Lambda$ , as follows :

$$\rho \xrightarrow{\Lambda} \sum_{i,j} \tilde{c}_{ij} |\Lambda s_i\rangle\langle \Lambda s_j|, \quad \tilde{c}_{ij} = \begin{cases} c_{ij} & \text{if } \Lambda s_i = \Lambda s_j, \\ c_{ij}/N & \text{otherwise.} \end{cases}$$

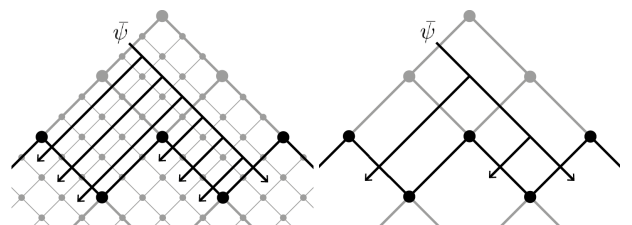


FIG. 9: Coarse-graining of a single  $\bar{\psi}$  at order  $\epsilon$ .  $N = 3$ . *Left* : the many arrows should be understood as a superposition of states. *Right* : the arrows are a mixture of states.  $N$  left moving states are mapped onto one coarse state.

Notice that, in the formal limit for  $N \rightarrow \infty$  the dynamics describes a fully classical propagation along the line, where the right- and left-moving coarse signals are completely decoupled. The most interesting case, is for finite  $N$ , where the effect of this coarse-graining map translates in renormalizing the coupling parameter  $m$ , embedded in the coherence terms of the density matrix, by a factor  $N$  :

$$m^{cg} = \frac{m}{N}.$$

In the continuous regime, this very dynamics which is fully captured by a Dirac equation in the microscopic substrate [30], with mass  $m$ , continues to be described by the same equation with a renormalised mass, due to a finite resolution. A straightforward calculation yields to :

$$\partial_t \rho = -i[H_D^{CG}, \rho]$$

which is still a Hamiltonian equation, with  $H_D^{CG} = i\sigma_z \partial_x - \sigma_x m^{cg}$ . Notice that the mass term scales as one over a length, which is usual in (continuous) field theory.

## V. CONCLUSION

We studied a color-blind QCA, following Goldilocks rules and we characterised its dual introducing extra qbits on the edges of the spacetime diagram. Such qbits plays the role of discrete gradient, accounting the difference, modulo 2, between neighbors qbits. We called them, signals. Such entities, propagates in spacetime and coincide formally with quantum walkers, living on the borders between region of different color. A new procedure to coarse-grain the overall microscopic system, has been introduced. We first partition the spacetime diagram in cells of size  $N$ . Then we project each cell on some probes on the borders. We found that it is possible to formally connect these probes to the signal dynamics, connecting them by a discrete analogous of the Stokes law. This yields a rigorous geometrical correspondence between the (edge) coarse-states and the microscopic (bulk) dynamics, which is reminiscent of the edge-bulk correspondence in quantum field theory. Finally we average via a CPTP map the cells, at different cell size  $N$ , leading to coarse dynamics. We showed that the emergent QCA still admits as continuous limit a Dirac free Hamiltonian, but with a renormalised mass, which scales inversely with the size of the cells, or in other terms with the resolution of the detector.

From a purely theoretical point of view, the direction is to generalise the previous results to QCA with interactions, as in [16]. The purpose is to provide new quantum simulation schemes for quantum field theories, taking into account the limited access that the observer has to the microscopic substrate. Also we may wonder whether the above results could be extended to higher dimensional space and in case of gauge field interaction. We leave it to future investigations.

## VI. ACKNOWLEDGEMENTS

The authors acknowledge inspiring conversations with Fernando de Melo, Pedro Costa who contributed to spark the idea of the first coarse-graining map in the context of Dirac QCA, Pablo Arrighi and Nathanael Eon for inspiring discussions on symmetries and invariances in QCA. This work has been funded by the Pépinière d'Excellence 2018, AMIDEX fondation, project DiTiQuS and the ID 60609 grant from the John Templeton Foundation, as part of the “The Quantum Information Structure of space-time (QISS)” Project.

## Appendix

## VII. COARSE-GRAINING MAP

Let us consider the quantum channel  $\Lambda$ , which maps fine states  $s$  onto coarse states  $S$  as follows :

$$\Lambda : |s\rangle\langle s| \rightarrow |S\rangle\langle S|.$$

Although the choice of  $\Lambda$  can be completely arbitrary, it has to be completely positive by definition, condition which is equivalent to the positivity of the Choi matrix  $C_\Lambda$  [31].

As an example, let us consider a fine state composed by two qbits  $|ef\rangle$  and its density matrix  $\rho = |ef\rangle\langle ef|$ . Our physical intuition may suggest us that (i) our detector is not good enough to distinguish, e.g., the states  $|01\rangle$  and  $|10\rangle$ , and (ii) that the population terms are preserved :

$$\begin{aligned} \Lambda(|00\rangle\langle 00|) &= |0\rangle\langle 0|; \\ \Lambda(|01\rangle\langle 01|) &= |1\rangle\langle 1|; \\ \Lambda(|10\rangle\langle 10|) &= |1\rangle\langle 1|; \\ \Lambda(|11\rangle\langle 11|) &= |1\rangle\langle 1|, \end{aligned}$$

where coherence terms are transformed as follow

$$\begin{aligned} \Lambda(|01\rangle\langle 00|) &= a|1\rangle\langle 0|; \\ \Lambda(|10\rangle\langle 00|) &= a|1\rangle\langle 0|; \\ \Lambda(|11\rangle\langle 00|) &= a|1\rangle\langle 0|; \end{aligned}$$

with  $a$  being a constant that we aim to constrain. The Choi matrix is a block matrix, with blocks  $(i, j)$ ,  $\Lambda(|i\rangle\langle j|)$ ,  $i, j$  being the element of the computational basis :

$$C_\Lambda = \begin{pmatrix} \begin{pmatrix} 1 & 0 \\ 0 & 0 \end{pmatrix} & \begin{pmatrix} 0 & a \\ 0 & 0 \end{pmatrix} & \begin{pmatrix} 0 & a \\ 0 & 0 \end{pmatrix} & \begin{pmatrix} 0 & a \\ 0 & 0 \end{pmatrix} \\ \begin{pmatrix} 0 & 0 \\ a^* & 0 \end{pmatrix} & \begin{pmatrix} 0 & 0 \\ 0 & 1 \end{pmatrix} & 0 & 0 \\ \begin{pmatrix} 0 & 0 \\ a^* & 0 \end{pmatrix} & 0 & \begin{pmatrix} 0 & 0 \\ 0 & 1 \end{pmatrix} & 0 \\ \begin{pmatrix} 0 & 0 \\ a^* & 0 \end{pmatrix} & 0 & 0 & \begin{pmatrix} 0 & 0 \\ 0 & 1 \end{pmatrix} \end{pmatrix} \quad (5)$$

Its non-null eigenvalues are  $\lambda = 1, 1, 1 \pm \sqrt{3aa^*}$  and they must be positive. Consequently,

$$|a| \leq 1/\sqrt{3},$$

which defines an upper bound for the coherence coefficients. Note that the choice  $a = 0$  translates in a projection onto the coarse states.

If we consider a more general coarse-graining onto  $L$  coarse states, where each coarse state corresponds to  $N$  fine states, matrix (VII) reads :

$$C_\Lambda \simeq \begin{pmatrix} \mathbf{1}_N & \mathbf{a} & \cdots & \mathbf{a} \\ \mathbf{a}^* & \mathbf{1}_N & \cdots & \mathbf{a} \\ \vdots & & \ddots & \\ \mathbf{a}^* & \mathbf{a}^* & \cdots & \mathbf{1}_N \end{pmatrix}.$$

The Choi matrix is now a block matrix whose  $L$  blocks have dimension  $N \times N$  and  $\mathbf{a}$  is a block filled with  $a$ . Again it must be positive. In particular, for  $a = 0$  its eigenvalues are all positive ; to study the general case, we use their analyticity in  $a$  and we look for a null eigenvalue ; this is equivalent to studying the  $L \times L$  matrix :

$$\begin{pmatrix} 1 & Na & \cdots & Na \\ Na^* & 1 & \cdots & Na \\ \vdots & & \ddots & \\ Na^* & Na^* & \cdots & 1 \end{pmatrix}.$$

After simple algebra, it is straightforward to verify that the spectrum of the above matrix is positive for a small set of  $a(N)$  encompassing 0, and that the maximum value coincides with  $a_{max} = 1/N$ .

Let

$$\rho = \sum_{i,j} c_{ij} |s_i\rangle\langle s_j|$$

be a fine grained density matrix and  $\Lambda$  be the uniform coarse-graining that gives the largest coherence ; then

$$\rho \xrightarrow{\Lambda} \sum_{i,j} \tilde{c}_{ij} |\Lambda s_i\rangle\langle \Lambda s_j|, \quad \tilde{c}_{ij} = \begin{cases} c_{ij} & \text{if } \Lambda s_i = \Lambda s_j, \\ c_{ij}/N & \text{otherwise.} \end{cases}$$

This shows that coarse-graining a quantum state reduces coherence and, then, the quantumness of the system. One can estimate this loss : coherence is divided by the cardinal  $N = \#\Lambda^{-1}$  ; it is as if the coherence of the coarse state were shared among its  $N$  fine states. Notice that this does not depend on  $L$  and this is also composable with respect to the iteration of coarse-graining. In the limit  $1/N \simeq 0$ , the system is fully classical.

---

[1] S. Wolfram, “Cellular automata as models of complexity,” *Nature*, vol. 311, no. 5985, pp. 419–424, 1984.

[2] A. Adamatzky, *Game of life cellular automata*, vol. 1. Springer, 2010.

[3] D. H. Rothman and S. Zaleski, *Lattice-gas cellular automata: simple models of complex hydrodynamics*, vol. 5. Cambridge University Press, 2004.

[4] B. S. Kerner, S. L. Klenov, and D. E. Wolf, “Cellular automata approach to three-phase traffic theory,” *Journal of Physics A: Mathematical and General*, vol. 35, no. 47, p. 9971, 2002.

[5] G. B. Ermentrout and L. Edelstein-Keshet, “Cellular automata approaches to biological modeling,” *Journal of theoretical Biology*, vol. 160, no. 1, pp. 97–133, 1993.

[6] B. Chopard in *Cellular Automata Modeling of Physical Systems*, pp. 407–433, Springer, New-York, 2012.

[7] J. Von Neumann and R. Kurzweil, *The computer and the brain*. Yale University Press, 2012.

[8] T. Neary and D. Woods, “P-completeness of cellular automaton rule 110,” in *Automata, Languages and Programming* (M. Bugliesi, B. Preneel, V. Sassone, and I. Wegener, eds.), pp. 132–143, Springer, Berlin, Heidelberg, 2006.

[9] P. Arrighi, “An overview of quantum cellular automata,” *Natural Computing*, vol. 18, pp. 885–899, 2019. arXiv:1904.12956v2.

[10] T. Farrelly, “A review of quantum cellular automata,” 04 2019. arXiv:1904.13318v1.

[11] P. Arrighi, G. Di Molfetta, I. Márquez-Martín, and A. Pérez, “Dirac equation as a quantum walk over the honeycomb and triangular lattices,” *Physical Review A*, vol. 97, no. 6, p. 062111, 2018.

[12] G. Di Molfetta, M. Brachet, and F. Debbasch, “Quantum walks as massless dirac fermions in curved space-time,” *Physical Review A*, vol. 88, no. 4, p. 042301, 2013.

[13] G. Di Molfetta and A. Pérez, “Quantum walks as simulators of neutrino oscillations in a vacuum and matter,” *New Journal of Physics*, vol. 18, no. 10, p. 103038, 2016.

[14] P. Arnault, G. Di Molfetta, M. Brachet, and F. Debbasch, “Quantum walks and non-abelian discrete gauge theory,” *Physical Review A*, vol. 94, no. 1, p. 012335, 2016.

[15] P. Arrighi, G. Di Molfetta, and N. Eon, “Gauge-invariance in cellular automata,” 2020. arXiv:1904.13318v1.

[16] P. Arrighi, C. Bény, and T. Farrelly, “A quantum cellular automaton for one-dimensional QED,” *Quantum Information Processing*, vol. 19, 2020. arXiv:1903.07007v1.

[17] P. Arnault, A. Pérez, P. Arrighi, and T. Farrelly, “Discrete-time quantum walks as fermions of lattice gauge theory,” *Physical Review A*, vol. 99, no. 3, p. 032110, 2019.

[18] P. Arrighi, S. Facchini, and M. Forets, “Discrete lorentz covariance for quantum walks and quantum cellular automata,” *New Journal of Physics*, vol. 16, 2014.

[19] A. Bisio, G. M. D’Ariano, and P. Perinotti, “Quantum walks, weyl equation and the lorentz group,” *Foundations of Physics*, vol. 47, no. 8, pp. 1065–1076, 2017.

[20] F. Debbasch, “Discrete geometry from quantum walks,” *Condensed Matter*, vol. 4, no. 2, p. 40, 2019.

[21] Y. Han, J. Jin, J. Wagner, and G. Voth, “Quantum theory of multiscale coarse-graining,” *Journal of chemical physics*, vol. 148, 2018.

[22] S. Bartlett, T. Rudolph, , and R. Spekkens, “Reference frames, superselection rules, and quantum information,” *Reviews of modern physics*, vol. 79, pp. 555–609, 2007. arXiv:quant-ph/0610030.

[23] O. Kabernik, “Quantum coarse-graining, symmetries and reducibility of dynamics,” *Phys. Rev. A*, vol. 97, 2018. arXiv:1801.09770v2.

[24] C. Agon, V. Balasubramanian, S. Kasko, and A. Lawrence, “Coarse grained quantum dynamics,” 2018. arXiv:1412.3148v4.

[25] J. Feret, V. Danos, J. Krivine, R. Harmer, and W. Fontana, “Internal coarse-graining of molecular systems,” *PNAS*, vol. 106, pp. 6453–6458, 04 2009.

[26] N. Israeli and N. Goldenfeld, “Coarse-graining of cellular automata, emergence, and the predictability of complex systems,” *Physical Review E*, vol. 73, no. 2, p. 026203, 2006.

[27] P. Costa and F. de Melo, “Coarse graining of partitioned cellular automata,” *arXiv preprint arXiv:1905.10391*, 2019.

[28] L. E. Hillberry, M. T. Jones, D. L. Vargas, P. Rall, N. Y. Halpern, N. Bao, S. Notarnicola, S. Montangero, and L. D. Carr, “Entangled quantum cellular automata, physical complexity, and goldilocks rules,” 05 2020. arXiv:2005.01763v1.

[29] V. Salo and I. Törmä, “Color blind cellular automata,” in *International Workshop on Cellular Automata and Discrete Complex Systems*, pp. 139–154, Springer, 2013.

[30] G. Di Molfetta and P. Arrighi, “A quantum walk with both a continuous-time limit and a continuous-spacetime limit,” *Quantum Information Processing*, vol. 19, no. 2, p. 47, 2020.

[31] M. A. Nielsen and I. Chuang, “Quantum computation and quantum information,” 2002.